

Dynamical Heating Induced by Dwarf Planets on Cold Kuiper Belt-like Debris Disks

M. A. Muñoz-Gutiérrez, B. Pichardo

*Instituto de Astronomía, Universidad Nacional Autónoma de México, Apdo. postal 70-264 Ciudad
Universitaria, México*

`mmunoz@astro.unam.mx`

M. Reyes-Ruiz

*Instituto de Astronomía, Universidad Nacional Autónoma de México, Apdo. postal 877, 22800 Ensenada,
México*

and

A. Peimbert

*Instituto de Astronomía, Universidad Nacional Autónoma de México, Apdo. postal 70-264 Ciudad
Universitaria, México*

ABSTRACT

With the use of long-term numerical simulations, we study the evolution and orbital behavior of cometary nuclei in cold Kuiper belt-like debris disks under the gravitational influence of dwarf planets (DPs); we carry out these simulations with and without the presence of a Neptune-like giant planet. This exploratory study shows that in the absence of a giant planet, 10 DPs are enough to induce strong radial and vertical heating on the orbits of belt particles. On the other hand, the presence of a giant planet close to the debris disk, acts as a stability agent reducing the radial and vertical heating. With enough DPs, even in the presence of a Neptune-like giant planet some radial heating remains; this heating grows steadily, re-filling resonances otherwise empty of cometary nuclei. Specifically for the solar system, this secular process seems to be able to provide material that, through resonant chaotic diffusion, increase the rate of new comets spiraling into the inner planetary system, but only if more than the ~ 10 known DP sized objects exist in the trans-Neptunian region.

Subject headings: planets and satellites: dynamical evolution and stability — Kuiper belt: general — methods: numerical

1. Introduction

One of the characteristics of evolved planetary systems is the prolonged presence of the remnants of stellar and planetary formation, ranging in size from dust grains to cometary nuclei to DPs. This material, located beyond the region where planets rapidly “clean-up” their vicinity, is known as a debris disk (for a review see Wyatt 2008; Kenyon et al. 2008, and references therein).

In our solar system the present day remnants in this region constitute the “Kuiper Belt” (KB). Although the lifetime of debris disks depends on diverse factors, such as the stellar mass and neighboring environment, the majority of 100 Myr old stars have observational features consistent with the presence of debris disks and even a few 10 Gyr old stars show evidence of having debris disks (Decin et al. 2003; Greaves et al. 2005).

The first discovered extrasolar debris disk was the one of Vega, detected by its infrared (IR) excess with the IRAS satellite (Aumann et al. 1984). The IR excess is believed to be produced by belts of dust particles originating from a steady collisional cascade (Müller et al. 2010); for the case of Vega, this belt is located at ~ 100 AU from the star. The study of extrasolar debris disks is relevant in several aspects to the understanding of the planetary system formation process; moreover, debris disks have been employed to determine the presence of planets in extrasolar planetary systems (Zuckerman & Song 2004).

On the other hand, DPs have an important role on the dynamics of primigenious planetary disks as the initiators of collisional cascades once they reach ~ 1000 to 3000 km size; they stir the orbits of residual icy planetesimals, increasing collisions; these collisions are responsible for both grounding some icy-planetesimals to dust, as well as creating some super-Earth sized cores (Kenyon & Bromley 2004, 2015). Also, massive planets in evolved debris disks are able to produce gaps and dust outflows (Moro-Martín & Malhotra 2005).

In the specific case of the KB, recent studies show that a number of its dynamical components can be explained with a migrating Neptune (e.g. Malhotra 1993; Levison & Morbidelli 2003; Chiang et al. 2007; Morbidelli et al. 2008; Nesvorný 2015). Indeed, all populations in the KB conserve evidences of their close interaction with the giant, except probably for the classical KB (CKB). The CKB has been defined as a bimodal orbital distribution: the hot (inclinations $i > 5^\circ$) and cold ($i < 5^\circ$) components (Brown 2001). However, some mixing between both populations seem to have taken place (Morbidelli et al. 2008; Volk & Malhotra 2011; Petit et al. 2011).

The most accepted scenario to explain the coexistence of both hot and cold populations (Batygin et al. 2011; Wolff et al. 2012; Nesvorný 2015) involves the action of a migrating Neptune, going outwards launching lots of planetesimals to form the hot population; the cold disk bodies, starting beyond 40 AU, simply kept their primordial orbits mostly unaffected by Neptune that stopped migrating at some point in the evolution of the early solar system when the disk material grew scarce (Gomes et al. 2004).

Regarding the largest bodies of the power spec-

tra on debris disks, the only examples we know are the KB objects (KBOs) with radii between 400 and 1200 km, a few of which have only recently been discovered (Brown et al. 2005). Extrapolation of the size distribution of smaller KBOs has sometimes been used to attempt to estimate the numbers of such larger objects (i.e. Bernstein et al. 2004), but estimations are still inconclusive.

Regardless of their number, it is usually believed DPs to have only a small influence on the evolution of debris disks in general. Fernández (1980) presents a first approximation where he attaches importance to massive objects, of up to $1.7 \times 10^{-4} M_\oplus$, in a very massive KB disk (about $9 M_\oplus$), finding that, in the presence of thousands of Ceres-like objects, direct encounters of cometary nuclei with larger bodies could lead to scatter of comets, sending them to the inner planetary region, in this way possibly maintaining a steady influx of short-period comets. Current estimates of the mass and composition of the KB rule out this possibility as the main driver to produce the observed population of short-period comets. The infall inrate of comets on planetary systems might be of great importance in terms of habitability for example: it is believed that a large fraction of the water in the primeval Earth came from comets and asteroids (Altwegg et al. 2015); also, at some later point it becomes necessary, for long-term evolution of life, to have a reduced cometary infall rate. However at present, other than the KB, we are not able to observe such details on other debris disks.

In this work we produce an exploratory study, that helps to better understand the dynamical effects of DPs on cold Kuiper belt-like debris disks (KBLDD) with and without the influence of a Neptune-like giant planet. The physical effects presented here are of a general nature, as such, we expect them to be relevant in a wide variety of debris disks. In particular, we believe these results can be qualitatively applied to the KB (although we do not pretend to present a detailed study of the KB dynamics). A more quantitative study of the KB or of any other specific debris disk is beyond the scope of this letter.

2. Simulations

In this work we explore by means of long-term numerical simulations, the influence of random DPs on the dynamics of cold KBLDDs. The random DPs share physical characteristics with the ones observed in the solar system’s trans-Neptunian region, while the cold KBLDDs resemble the observed cold population of the solar system’s CKB. We constructed our initial conditions to resemble the cold CKB because it is the component least affected by Neptune, therefore the most stable. This is also the most intuitive starting point for a generic statistical study of debris disks. Among the differences with the solar system precise conditions are: the exact quantity of DPs, a zero inclination for our Neptune-like giant planet, and the random generated initial conditions of the belt particles.

For our studies we employ the hybrid symplectic integrator included in the MERCURY package (Chambers 1999). This integrator lets us follow the evolution of test particles in a potential generated by several major N-bodies plus a central star. It also permits to follow close encounters between bodies with high accuracy by switching from a symplectic to a Bulirsh-Stöer integrator; the switch between integrators takes place when particles get closer than a limit imposed in terms of the given major body’s Hill radius ($R_H = (M_p/3M_\odot)^{1/3}$).

All simulations are 1 Gyr long with an accuracy tolerance for the Bulirsh-Stöer integrator of 10^{-10} , a changeover distance between integrators of $3R_H$ for any major body, and a time-step of 180 days for the symplectic integrator. The simulations were performed on *Atocatl*¹.

2.1. Major Bodies

The main central body in all simulations is a $1 M_\odot$ star.

We consider 4 different initial DP configurations: we use 10, 30, 50, and 100 randomly generated cold DPs. The orbital parameters of all DPs lie within the following limits: semimajor axes, $35 \text{ AU} < a < 60 \text{ AU}$; eccentricities, $0.0 < e < 0.1$; inclinations, $0.0^\circ < i < 5.0^\circ$; arguments of peri-

center, $0^\circ < \omega < 360^\circ$; longitudes of the ascending node, $0^\circ < \Omega < 360^\circ$; and mean anomalies, $0^\circ < M < 360^\circ$. DP masses take random values in the range $3.3 \times 10^{-6} M_\oplus < m < 2.8 \times 10^{-3} M_\oplus$, where upper limit corresponds to Eris’s mass, while the lightest corresponds to the mass of 2002 AW₁₉₇, this is, the biggest and one small but significant object in our trans-Neptunian region.

All four DP configurations were run with and without the presence of a giant planet. The parameters for this body were exactly the ones the real Neptune has but with zero inclination for the sake of simplicity, because the giant planet defines the angular momentum of the system (i.e. this represents the natural reference system of the problem); had we chosen different planes for the giant planet and the KBLDD an initial rearrangement of test particles would have occurred to come into balance with the giant planet’s plane.

To better see the cumulative effect, we constructed the sets of DPs in such a way that the larger DP sets include all the DPs of the previous set, i.e. the set of 10 DPs is a subset of the one of 30 DPs, etc. The total mass in DPs for 10, 30, 50, and 100 objects is respectively: 0.011, 0.032, 0.063, and $0.131 M_\oplus$; for comparison, the CKB estimated mass is $\sim 0.01 M_\oplus$ (Bernstein et al. 2004; Fraser et al. 2014).

2.2. Test particles’ initial conditions: Random Cold KBLDD

We generate a belt of 1000 test particles that resemble the observed cold CKB population. According to Kavelaars et al. (2008), Petit et al. (2011), and Dawson & Murray-Clay (2012), the current cold CKB have orbits with semi-major axes, $42.5 \text{ AU} < a < 44.5 \text{ AU}$, but mainly around 44 AU, with inclinations, $i < 4^\circ$, and eccentricities, $e < 0.05$, for most objects of the population.

We assign the values of the orbital parameters of the particles as follows: for a we use a random Gaussian distribution with mean and standard deviation: $\langle a \rangle = 44.0 \text{ AU}$, $\sigma_a = 1.5 \text{ AU}$. For e and ω we generate a point distribution in an XY plane where each coordinate gets random Gaussian values with mean zero and standard deviations given by $\sigma_{(e_X, e_Y)} = 0.03$; each point represents a vector, $\vec{e} = (e_X, e_Y)$, whose magnitude, $|\vec{e}| = \sqrt{e_X^2 + e_Y^2}$, is the e of the particle; also, we define the an-

¹*Atocatl* is a supercomputer of the Instituto de Astronomía at UNAM.

gle between \vec{e} and the X axis, ϕ_e , as ω , therefore $\omega = \phi_e = \text{Tan}^{-1}(e_Y/e_X)$; in this manner the initial e distribution has mean and standard deviation: $\langle e \rangle = 0.037$, $\sigma_e = 0.019$, while ω is randomly distributed between 0° and 360° . We follow an analogous procedure to obtain the i and Ω distributions; in this case we generate coordinates with random Gaussian points with mean zero and standard deviations given by $\sigma_{(i_X, i_Y)} = 1.2^\circ$; the resulting i follows a distribution with $\langle i \rangle = 1.52^\circ$, $\sigma_i = 0.80^\circ$; while Ω is randomly distributed between 0° and 360° . Finally, for M we use random values between 0° and 360° .

3. Results and Discussion

Fig. 1 shows the initial and final distributions of test particle eccentricities (left panel) and inclinations (right panel) in the simulations without a Neptune-like giant planet; the black line represents the initial conditions, while the different shades of blue represent the final distributions for 10, 30, 50, and 100 DPs. Analogously, Fig. 2 shows the same distributions when, along with the DPs, a Neptune-like planet is included at 30.09 A.U.

From Fig. 1 we see that both e and i shift toward larger values as the number of DPs increases; this is to be expected as more DPs will produce a larger number of close encounters with test particles, resulting in larger dispersions of e and i . A striking difference between e and i distributions can be noted: while for e there are more disturbed particles as the number of DPs increases; for i there seems to exist a saturation limit, where no particles can be heated beyond $\sim 11^\circ$, not even with 100 DPs, while the mean of the distribution remains near $\sim 5^\circ$ with 30, 50, and 100 DPs. The latter is result of the initial distribution of DPs; as they are cold, with maximum initial inclinations of 5° , they do not seem to be able to push test particle's i far beyond this limit. With 10 DPs there is less dynamical heating and this limit is not reached, remaining around 4° .

An interesting effect occurs when a Neptune-like planet is included in the simulations: as seen in Fig. 2, scattering induced by 10 and 30 DPs is severely damped for both e and i distributions. Again, with increasing DPs number, scattering of particles becomes stronger, leading to a shift of the distributions to higher values of e and i . For 50

and 100 DPs, damping is slightly less important and, although fewer in number, some particles can rise to values of 0.20 and 11° for e and i , respectively (values similar to the ones reached without a giant planet). Again, the mean values of the final i distributions grow with DPs number, but always remain below 5° ; even with 100 DPs, the mean is $\sim 4^\circ$. This implies, contrary to intuition, that a giant planet can act as a stabilizing agent, by helping to vertically bound particles in its gravitational potential (see Fig. 3). Mechanisms that could be responsible for this effect are: a) a suppression on the number of close encounters of the cometary nuclei with DPs induced by the giant planet; from our studies we find an opposite behavior, i.e. the presence of a giant planet increases the number of collisions due to the higher disk density produced by its presence. b) Resonances with the giant; in this case, mean motion resonances (MMR) in the plane of the disk produced by the giant have a strong influence very high above the disk plane, flattening considerably the disk; this phenomenon has been recently demonstrated to occur in galactic disks (Moreno et al. 2015), however the lack of filamentary structure on Fig. 3, may suggest this effect is not important. c) Resonances induced by the DPs on the cometary nuclei; in this case the giant planet breaks the phases of the particle-DP interaction preventing the more efficient resonant heating. d) A gravitational non-resonant origin based only on the vertical force exerted by the giant; on average the giant acts like a 30 AU ring that pulls the cometary nuclei towards the plane of the disk producing the distinctive triangle-like shape seen in Figure 3.

With enough DPs, the effect of very close encounters with DPs will be able to overcome the stabilizing influence of the giant planet; clearly, there must be a limit on how far this stabilizing influence can be exerted, but in the radii we explore, we do not reach it. In the presence of the giant, there are more close encounters due to the higher density; this may lead to more dust production in the disk than without the presence of the giant.

The left panels of Fig. 4 show the evolution throughout the simulations of $\langle e \rangle$ and $\langle i \rangle$, while the right panels show σ_e and σ_i , respectively. Broad lines show the evolution produced by DPs without a giant planet, while thin lines correspond

to simulations that include a Neptune-like body. The top-left panel of Figure 4 shows how, in all 8 cases, $\langle e \rangle$ increases almost monotonically; naturally, as the number of DPs increases, their effect on the final $\langle e \rangle$ increases. The top-right panel shows a similar behavior for σ_e (note the different scale between panels). These results strengthen what we have seen in the previous figures: the increasing presence of minor bodies increasingly perturbs the test particles, both with and without a giant planet.

The growing radial heating allows test particles to encounter resonances, replenishing them with cometary nuclei. This effect is clear in spite of the small number of test particles we employ in our simulations. This becomes relevant not only because of the inherently fascinating behavior of particles trapped into resonances, but also because it is generally assumed that, in advanced stages of debris disks, there are no more known mechanisms able to restock the material on resonant regions.

We also find that several of those particles are effectively trapped by resonances with the giant planet increasing dramatically their eccentricities. This mechanism might work as a plausible secular process able to sustain a rate of new comets spiraling into the inner planetary system (this rate has not been fully explained for the KB).

By comparing the thin to the broad lines in the two bottom panels of Fig. 4, we can see the stabilizing effect of a Neptune-like planet: without the giant planet $\langle i \rangle$ quickly grows to reach the 5° limit found before, when a Neptune-like body is present evolution is smooth and rising but slower; with a giant planet, 100 DPs are required to produce a similar effect to what 10 DPs were able to achieve without the giant. Also, without a giant planet, 30 DPs are enough to get close to some sort of saturation point, and there is very little difference between the final values for $\langle i \rangle$ for 50 and 100 DPs; the saturation value seems to be similar to the DPs inclination initial distribution.

A similar trend is observed in the σ_i evolution: the maximum dispersion reached is about 2.1° for 30, 50, and 100 DPs without a giant planet, while with the giant this limit is about 1.6° . The effect produced by 10 bodies without the giant planet, clearly seen in both $\langle i \rangle$ and σ_i , almost disappears in the presence of the giant planet. In our solar system around 10 objects comparable in size

to Pluto have been discovered, if this is the total number of this kind of bodies, their effect on our KB would be hardly noticeable; however, there is the possibility that the total number of DPs is several times larger.

4. Conclusions

With the use of long-term, N-body numerical simulations we have studied the dynamical effect of DPs on a cold debris disk with and without the presence of a giant planet.

In the absence of the giant, DPs require only 1 Gyr to induce substantial vertical heating on initially cold test particles; this process increases the inclinations up to a saturation value of the order of the highest initial DP inclinations, in our simulations, 5° . Likewise, radial heating (eccentricity dispersion) increases rapidly, although in this case, saturation is not reached.

On the other hand, in the presence of a Neptune-like giant planet, the contribution of the DPs to the general heating diminishes severely. The 5° inclination limit obtained without the giant planet is no longer reached, not even with 100 DPs; in this case, the giant planet acts as a stability agent, concerning particle inclinations specifically, reducing the vertical heating. Regarding the radial heating, albeit a reduction is also observed, significant heating remains and grows steadily in time. The gravitational influence of the giant planet prevents the particles from dispersing, keeping a higher density on the disk; this may have important consequences on the rate of collisions and on dust production.

Another consequence of the heating produced by DPs is a slow but constant secular radial migration of particles in the belt; several of those particles are eventually trapped in the giant planet's MMRs where, through chaotic diffusion, they could become part of other dynamical families (e.g. Centaurs; Tiscareno & Malhotra 2009).

The continuous replenishing of resonant regions with new cometary nuclei leads several particles through a dynamical evolution process that produces close encounters with the giant planet. Those bodies contribute to the influx rate of new short-period comets that may become important from the point of view of habitability, however observations of this mechanism are not yet avail-

able for planetary systems other than our Kuiper belt. In the case of the solar system this mechanism may contribute to the short-period comet influx rate, in better accordance with observations (Emel'yanenko et al. 2005; Volk & Malhotra 2008, 2013); this is assuming the possibility of the existence of more than ten DPs in the trans-Neptunian region. Moreover, if the formation of several tens of DPs in the outer regions of our solar system took place prior to the migration of Neptune, a vertically pre-heated debris disk could have been already present when Neptune reached its current location; such process would produce a soft mixing between: the cold CKB population, the hot CKB population, and the resonant objects (those swept during Neptune's migration).

Authors are grateful to A. Morbidelli, R. Malhotra and our anonymous referee for valuable comments. We acknowledge support from UNAM-PAPIIT grants IN-114114, IN-115413, and CONACyT grant 241732. M.A.M. thanks support from CONACyT scholarship for conducting PhD studies.

REFERENCES

- Altwegg, K., Balsiger, H., Bar-Nun, A., et al. 2015, *Science*, 347, 1261952
- Aumann, H. H., Beichman, C. A., Gillett, F. C., et al. 1984, *ApJ*, 278, L23
- Batygin, K., Brown, M. E., & Fraser, W. C. 2011, *ApJ*, 738, 13
- Bernstein, G. M., Trilling, D. E., Allen, R. L., et al. 2004, *AJ*, 128, 1364
- Brown, M. E. 2001, *AJ*, 121, 2804
- Brown, M. E., Trujillo, C. A., & Rabinowitz, D. L. 2005, *ApJ*, 635, L97
- Chambers, J. E. 1999, *MNRAS*, 304, 793
- Chiang, E., Lithwick, Y., Murray-Clay, R., et al. 2007, *Protostars and Planets V*, 895
- Dawson, R. I., & Murray-Clay, R. 2012, *ApJ*, 750, 43
- Decin, G., Dominik, C., Waters, L. B. F. M., & Waelkens, C. 2003, *ApJ*, 598, 636
- Emel'yanenko, V. V., Asher, D. J., & Bailey, M. E. 2005, *MNRAS*, 361, 1345
- Fernández, J. A. 1980, *MNRAS*, 192, 481
- Fraser, W. C., Brown, M. E., Morbidelli, A., Parker, A., & Batygin, K. 2014, *ApJ*, 782, 100
- Gomes, R. S., Morbidelli, A., & Levison, H. F. 2004, *Icarus*, 170, 492
- Greaves, J. S., Holland, W. S., Wyatt, M. C., et al. 2005, *ApJ*, 619, L187
- Kavelaars, J., Jones, L., Gladman, B., Parker, J. W., & Petit, J.-M. 2008, *The Solar System Beyond Neptune*, 59
- Kenyon, S. J., & Bromley, B. C. 2004, *AJ*, 127, 513
- Kenyon, S. J., Bromley, B. C., O'Brien, D. P., & Davis, D. R. 2008, *The Solar System Beyond Neptune*, 293
- Kenyon, S. J., & Bromley, B. C. 2015, *ApJ*, 806, 42
- Levison, H. F., & Morbidelli, A. 2003, *Nature*, 426, 419
- Malhotra, R. 1993, *Nature*, 365, 819
- Morbidelli, A., Levison, H. F., & Gomes, R. 2008, *The Solar System Beyond Neptune*, 275
- Moreno, E., Pichardo, B., & Schuster, W. J. 2015, *MNRAS*, 451, 705
- Moro-Martín, A., & Malhotra, R. 2005, *ApJ*, 633, 1150
- Müller, S., Löhne, T., & Krivov, A. V. 2010, *ApJ*, 708, 1728
- Nesvorný, D. 2015, arXiv:1504.06021
- Tiscareno, M. S., & Malhotra, R. 2009, *AJ*, 138, 827
- Volk, K., & Malhotra, R. 2008, *ApJ*, 687, 714
- Volk, K., & Malhotra, R. 2011, *ApJ*, 736, 11
- Volk, K., & Malhotra, R. 2013, *Icarus*, 224, 66
- Petit, J.-M., Kavelaars, J. J., Gladman, B. J., et al. 2011, *AJ*, 142, 131

Wyatt, M. C. 2008, *ARA&A*, 46, 339

Wolff, S., Dawson, R. I., & Murray-Clay, R. A.
2012, *ApJ*, 746, 171

Zuckerman, B., & Song, I. 2004, *ApJ*, 603, 738

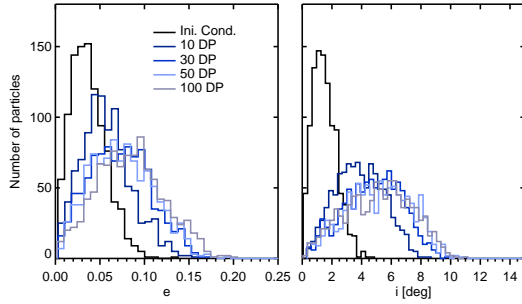


Fig. 1.— Initial and final distributions of test particles. Left panel shows the initial e distribution of KBLDD particles (black line) and the final distributions, after 1 Gyr evolution, when 10 (darker blue line), 30 (middle blue line), 50 (lighter blue line), and 100 (gray line) random DPs are present in the simulation. Right panel is the same but for i .

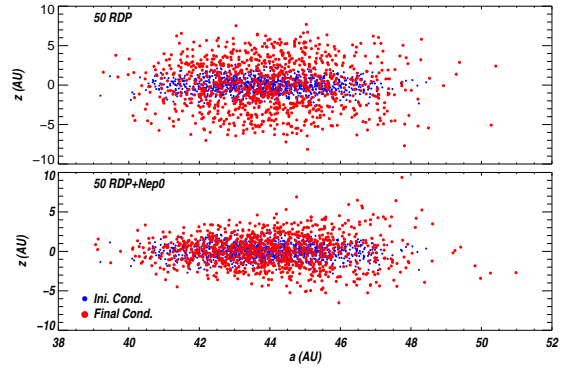


Fig. 3.— Height over the plane (z) vs. semimajor axis (a). The upper panel shows the cometary nuclei initial conditions (blue) and final (red) for our run with 50 DPs and no giant planet. Lower panel shows the same but for the run with 50 DPs plus the giant.

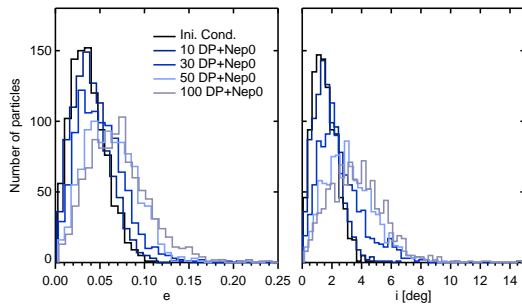


Fig. 2.— Same as Fig. 1 but including a Neptune-like giant planet at 30.09 A.U.

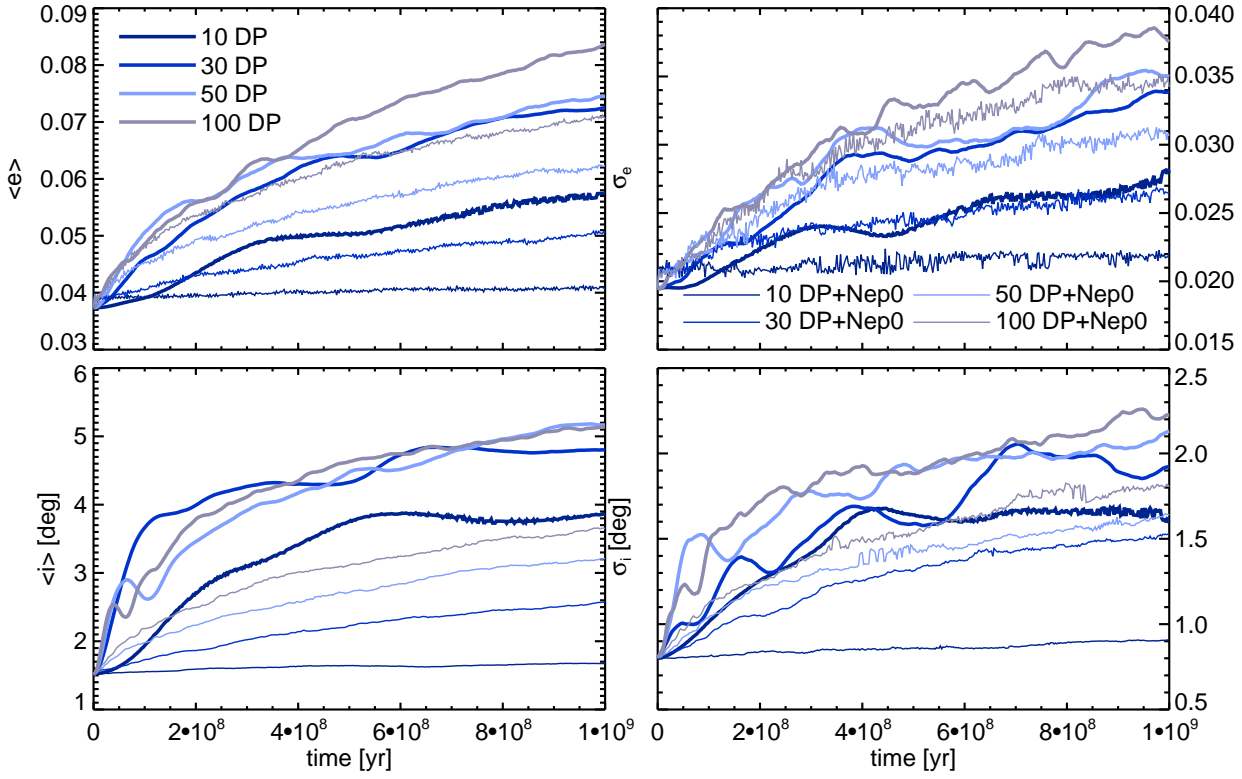


Fig. 4.— Evolution of test particle averages and standard deviations for eccentricity and inclination: top-left panel shows $\langle e \rangle$, top-right panel shows σ_e , bottom-left shows $\langle i \rangle$, and bottom-right shows σ_i . Broad lines stand for simulations without a giant planet, while thin lines for simulations that include a Neptune-like planet. Color code is the same as in Fig. 1.